International Journal of High-Rise Buildings
September 2015, Vol 4, No 3, 171-180

International Journal of
High-Rise Buildings
www.ctbuh-korea.org/ijhrb/index.php

Collapse Behavior of an 18-Story Steel Moment Frame during a Shaking Table Test

Keiichiro Suita[1,†], Yoshitaka Suzuki[2], and Motomi Takahashi[3]

[1]*Department of Architecture and Architectural Engineering, Kyoto University, Kyoto, Japan*
[2]*Structural Research Department, Kobori Research Complex Inc., Tokyo 107-8502, Japan*
[3]*Building Structures Group, Kajima Technical Research Institute, Kajima Corporation, Tokyo 182-0036, Japan*

Abstract

A shaking table test was conducted at the E-Defense shaking table facility to investigate the damage and collapse behavior of a steel high-rise building under exceedingly large ground motions. The specimen is a one-third scale 18-story steel moment frame designed and constructed according to design specifications and practices used in the 1980s and 1990s. The shaking table tests used a long-duration, long-period ground motion simulated for a sequential Tokai, Nankai, and Nankai earthquake scenario. The building specimen was subjected to a series of progressively increasing scaled motions until it completely collapsed. The damage to the steel frame began through the yielding of beams along lower stories and column bases of the first story. After several excitations by increasing scaled motions, cracks initiated at the welded moment connections and fractures in the beam flanges spread to the lower stories. As the shear strength of each story decreased, the drifts of lower stories increased and the frame finally collapsed and settled on the supporting frame. From the test, a typical progression of collapse for a tall steel moment frame was obtained, and the hysteretic behavior of steel structural members including deterioration due to local buckling and fracture were observed. The results provide important information for further understanding and an accurate numerical simulation of collapse behavior.

Keywords: High-rise steel building, Shaking table test, Long-period ground motion, Collapse behavior, Fracture of moment connection

1. Introduction

Many brittle fracture of welded moment connections observed in the 1994 US Northridge Earthquake and 1995 Japan's Hyogoken-Nanbu Earthquake disclosed weaknesses of steel moment resisting frames. Development of more reliable connections was a key for providing better seismic performance of steel building structures. After extensive studies in US and Japan, since various modification was adopted concerning electrodes, ductility of steel, connection details and welding practice, the deformation capacity of steel connections was remarkably improved to prevent brittle fracture (Suita et al., 2000).

Although brittle fracture can be avoided by these efforts, the possibility of ductile fracture of connections is still remained under repeated plastic deformation. Recent advancement of prediction methods has enabled precise computation of long-period and long-duration ground motions produced by offshore earthquake such as the Nankai Trough Earthquake in Japan. The characteristics of these ground motions are different from motion records by near fault earthquakes such as Northridge or Hyogoken-Nanbu Earthquake. The predominant periods are longer by two second or more and the duration of motion can be as long as ten minutes or so. Therefore, the response of high-rise buildings against long-period ground motions is drawing attention (Suita et al., 2014). The 2011 Great East Japan Earthquake was a typical ocean-trench earthquake and many tall buildings in Tokyo metropolitan area were strongly shaken (Kasai et al., 2012). For a tall building constructed by steel structure, it is necessary to evaluate the deformation capacity until ductile fracture of moment connections subjected to a very large number of cyclic deformation in plastic range.

Another important issue concerning steel moment frames is the possibility of collapse of frames which sustained fracture at beam-to-column connections. In case of the Northridge and the Hyogoken-Nanbu Earthquakes, none of frames collapsed in spite of many brittle fracture of beams, residual deformation of those frames were quite small without being noticed in many cases. If a high-rise moment frame sustained many fracture at the beams, the greatest concern is the possibility of collapse of the frame during long-period and long-duration ground motions.

As a response to lessenes learned from the 2011 Great East Japan Earthquake about the potential intensity of large

[†]Corresponding author: Keiichiro Suita
Tel: +81-75-383-2948; Fax: +81-75-383-2948
E-mail: suita@archi.kyoto-u.ac.jp

offshore earthquakes, a project has been initiated entitled "Special Project for the Maintenance and Recovery of Functionality in Urban Infrastructure" in 2012. One of the main focus points of this project is qualification of collapse margins in high-rise buildings and a shaking table test of a 18-story steel high-rise building was conducted. This paper presents damage and processe to collapse of a frame observed in the test.

2. Building Specimen and Ground Motion

2.1. Building specimen

The building specimen is a one-third scale 18-story steel moment frame whose plan dimension is 5×6 m, and the total height is 25.35 m (Fig. 1). The total weight of the specimen is 3800 kN (not including foundation). The scale of the specimen is decided due to the limitation and capacity of the E-Defense facility. The structural characteristics of one-third scale structural components are examined by special element experiments and compaered with the behavior of corresponding full-scale specimens. From results of peliminary experiments, it is confirmed that the restoring force characteristics and plastic deformation capacity including deterioration by local buckling or fracture of steel elements are identical between one-third scale specimens and full-scale spesimens.

The steel frame is designed and constructed according to design specifications and practices in date from 1980s to 1990s. The baseshear coefficient of the frame at the plastic collapse mode defined by plastic hinges at beam ends is 0.45. This value is somewhat larger than design level because the sections of main members are increased to satisfy the requirement of maximum drift to be less than 0.01 rad.

In those days, any seismic dampers are hardly used and energy dissipation of a steel frame is expected under strong ground motions. In order to secure stable energy dissipation performance of the frame, beams and columns are designed to possess small enough width-to-thickness ratio and the column overdesign ratio is more than 1.50. Built-up square tube columns are used from 1st to 7th story and cold-formed square tube columns are used from 8th to 18th story. Wide-flange section of beams are connected to columns by site-welding method, i.e., flange-welded and web-bolted type and adequate diaphragm plates are inserted in the section of square tube columns at the location of the joint with flanges of beams. The details of welded moment connections (Fig. 2) and welding practices were typical style before the 1995 Hyogoken-Nanbu Earthquake. The style of the steel frame adopted in the specimen was commonly used for high-rise buildings in those days. The grade of steel of specimen is SM490A, whose nominal yield strength is 325 N/mm^2 and tensile strength is 490 N/mm^2. The fracture toughness of beams obtained from CV test is 200 J at 0ºC, which is high quality to prevent brittle fracture.

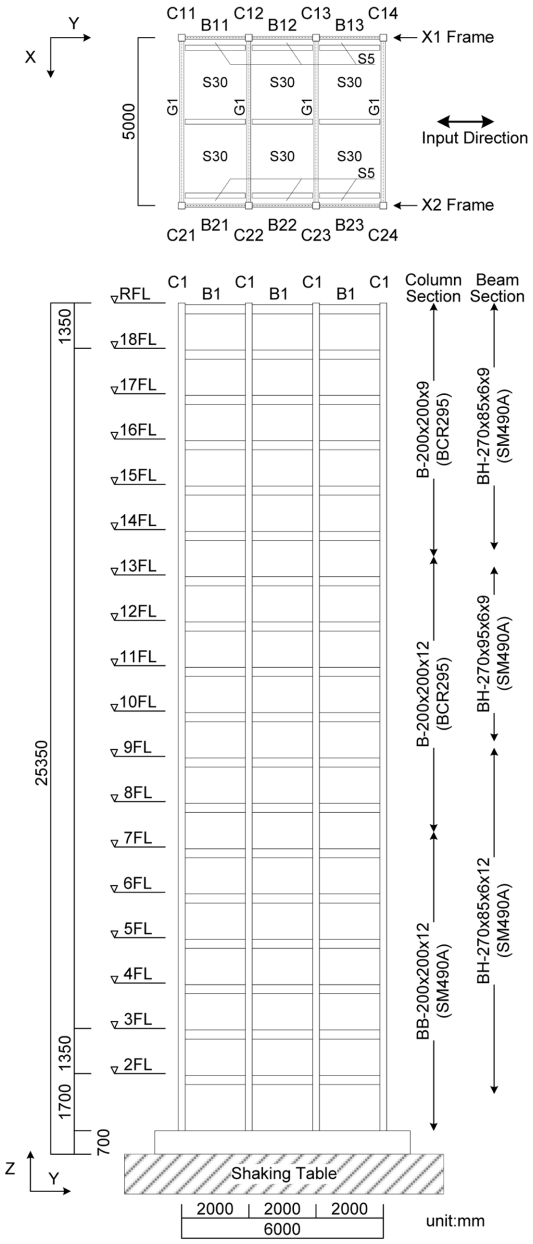


Figure 1. Specimen frame.

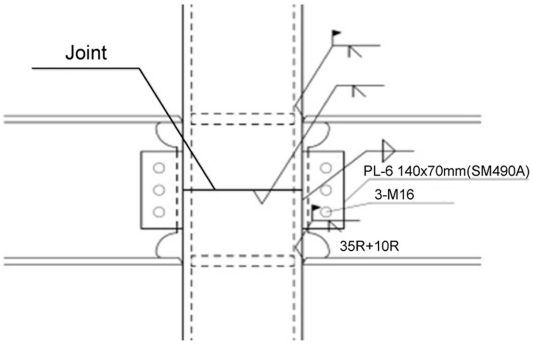


Figure 2. Beam-to-column connection (2-7F).

The specimen consists of two parallel three-bay plane frames connected by beams in the orthogonal direction. The shake of the table is conducted in one direction which is parallel to the direction of two plane test frames. Therefore, bi-axial behavior of the frame and columns are not examined in this experiment. A reinforced concrete slab, 50 mm depth, is settled on each floor and joined with beams by stud bolts to obtain sufficient in-plane stiffness of the floor and the composite action with beams. The total weight of the floor is set as 7 kN/m^2 and in order to properly simulate gravity and inertia forces, additional concrete plates suspended under the floor slab. The ratios of axial force to yield strength of the column are 0.12 (outer column) and 0.16 (inner column) by longtime load and 0.58 and 0.52 during seismic response at the first story. By using flexural full plastic strength of columns considering axial force, the column overdesign ratio during seismic response is 1.53 to 1.62, which is almost the same as the design target value. The safeguard frame is used to protect the shaking table from damage during collapse test. This frame has sufficient stiffness to be regarded as rigid.

2.2. Input ground motion

A long-period long-duration ground motion is generated on the assumption of coinstantaneous earthquakes of Tokai, Tonankai and Nankai Earthquake whose seismic center is located at Nankai Trough.

Synthetic 2100 ground motions are computed according to the method proposed by Ministry of Land, Infrastructure, Transport and Tourism in December 2010. The target spectrum is decided as the average of psude velocity spectrum (damping factor is 0.05) of 2100 calculated ground motinos. The records obtained at Tokyo during 2011 Great East Japan Earthquake is used as the phase of the ground motion.

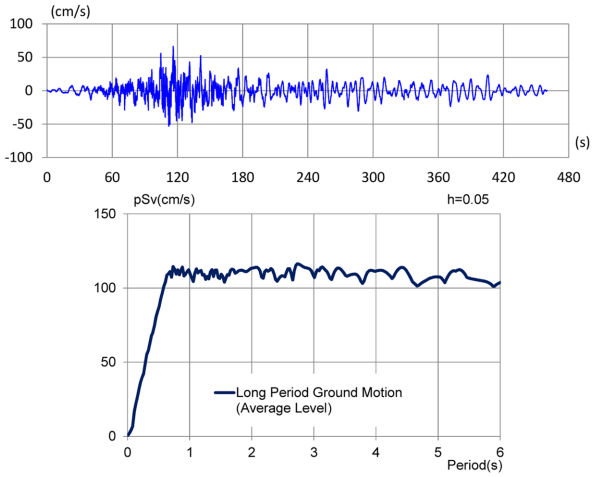


Figure 3. Velocity time history and pseudo velocity response spectrum of input ground motion.

The velocity time history and pseude velocity response spectrum is shown in Fig. 3. The maximum velocity is about 65 cm/s, duration is 460 seconds, maximum pseudo response velocity ${}_pS_v$, under 0.05 damping factor, is 110 cm/s and the response characteristics is almost flat between 0.6 and 10 second. The maximum pseudo response velocity of 2100 computed ground motions is 180 cm/s. In the shaking test, the time scale of the ground motion is shortened to $1/\sqrt{3}$ based on similitude laws. The ground motion intensity is incremented from design level to over maximum level until collapse occurs. In this paper, the

Table 1. Result of shaking table test

Test	Input level		Description of input level	Max. disp. at the top (cm)	Max. story drift angle (floor)	Damage to specimen
	${}_pS_v$ (cm/s)	% to pSv110				
pSv40	40	36.4	Design level 1	8.5	1/171 (14F)	None (elastic)
pSv80	81	73.6	Design level 2	15.3	1/110 (3,14F)	Full plastic of beam end (2-4F)
pSv110-1	110	100.0	Average of prediction	20.6	1/90 (14F)	Full plastic of beam end (2-7F) and column base (2-5F)
pSv110-2	110	100.0	Average of prediction	21.7	1/91 (14F)	ditto
pSv180-1	180	163.6	Max. of prediction	30.8	1/62 (11F)	Full plastic of beam end (2-14F), Crack initiation beam end (2-5F)
pSv180-2	180	163.6	Max. of prediction	31.7	1/55 (11F)	Crack progress beam end (2-5F)
pSv220	220	200.0	Over max. of prediction	34.7	1/48 (9F)	Fracture of beam flange (2F)
pSv250	250	227.3	Over max. of prediction	33.7	1/45 (2F)	Fracture of beam flange (2-3F)
pSv300	300	272.7	Over max. of prediction	37.4	1/30 (2F)	Fracture of beam flange (2-5F)
pSv340-1	340	310.0	Over max. of prediction	51.0	1/16 (2F)	Fracture of beam flange (upper Fl.) Local buckling of column base (1F)
pSv340-2	340	310.0	Over max. of prediction	56.3	1/13 (2F)	ditto
pSv420-1	420	381.8	Over max. of prediction	66.6	1/10 (2F)	Total fracture of beam end (2-5F)
pSv420-2	420	381.8	Over max. of prediction	100.0	1/6 (2F)	Fracture of column base (1F)
pSv420-3	420	381.8	Over max. of prediction	Collapse	Collapse	Collapse



Figure 4. Collapse of lower stories (pSv420-3).

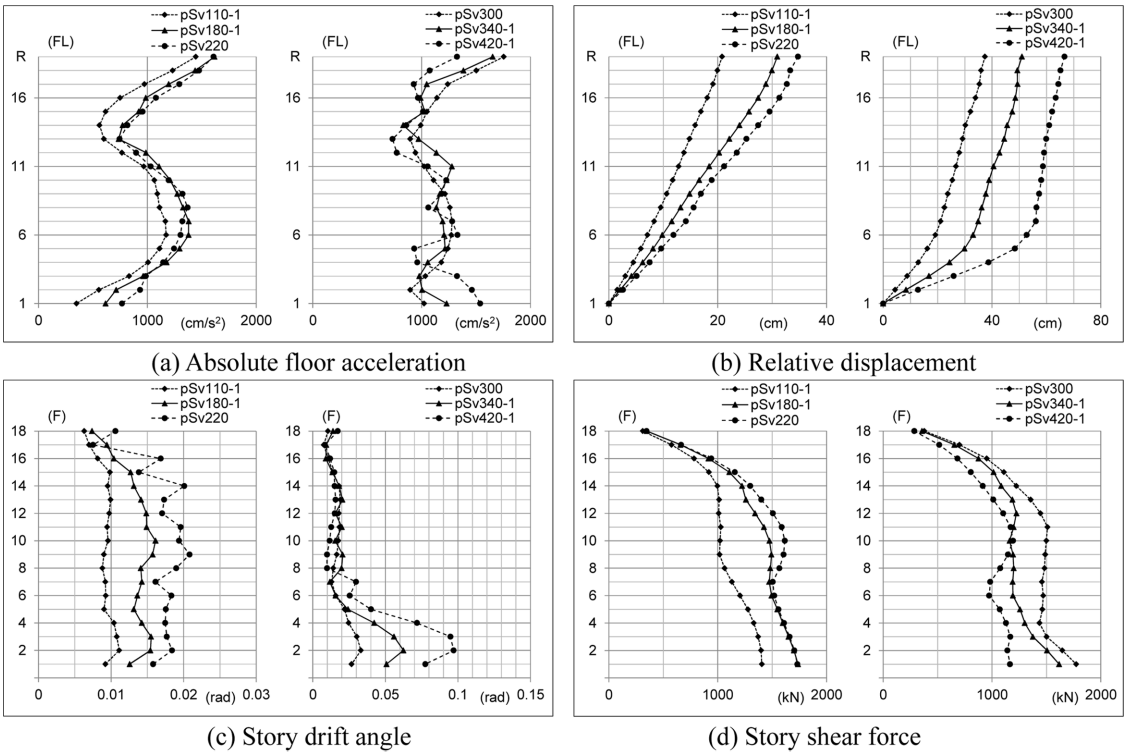
intensity of input motion is expressed by ${}_pS_v$ and the maximum ${}_pS_v$ is 420 cm/s at the final excitation.

3. Response of Specimen Frame

3.1. Overall behavior

Results of shaking table tests, namely, input level, maximum response and damage to the specimen are summarized in Table 1. The input level of ground motion started at the smallest ${}_pS_v$ 40 cm/s and finalized at the maximum ${}_pS_v$ 420 cm/s. In this paper, behavior of specimen are indicated about the selected input levels, i.e., pSv110-1, 180-1, 220, 300, 340-1, 420-1. During the pSv420-3 test, the specimen frame collapsed at the lowest four stories as shown in Fig. 4.

The oberall behavior are indicated in Fig. 5. The profile of absolute acceralation (Fig. 5(a)) shows both of 1st and 2nd mode shape until the pSv220 test. As the input level increases, the 2nd mode component decreases and the acceleration becomes close to uniform distribution after the pSv300 test. The profile of relative displacement (Fig. 5(b)) shows almost linear increase of displacement along height until the pSv220 test, but after the pSv300 test, displacement concentrated at 1st to 6th stories. The profile of story drift angle (Fig. 5(c)) shows almost uniform distribution until the pSv220 test, subsequently drift angle increases at only lower stories 1st to 5th stories and drift angle of upper stories fixed about 1/50 rad. The profile of story shear force (Fig. 5(d)) shows parallel increase along



(a) Absolute floor acceleration

(b) Relative displacement

(c) Story drift angle

(d) Story shear force

Figure 5. Profile of maximum response.

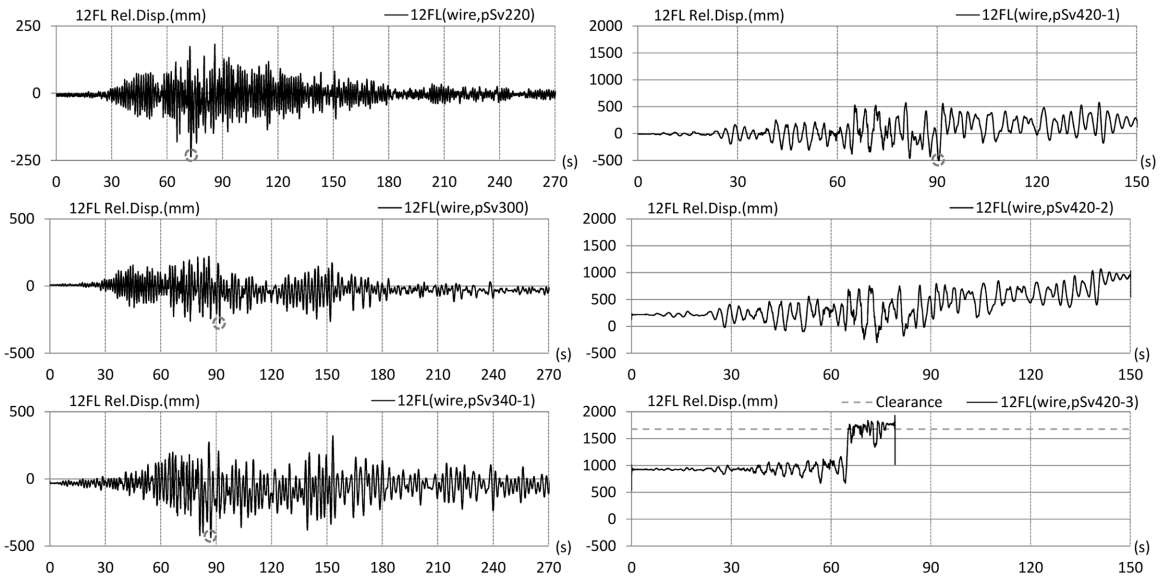


Figure 6. Time history of relative displacement at the 12th floor.

with input level until the pSv300 test, after that decrease due to deterioration by fracture and local buckling at plastic hinges of main structural components and increase of PΔ effect.

The time histories of the 12th floor which corresponds to the equivalent height of the frame are shown in Fig. 6. Until the pSv220 test, the maximum drifts of floor increased and residual displacement was hardly observed. After the pSv300, dynamic response characteristics of the frame changed, the instant of the maximum displacement changed and extension of the natural period was observed according to the increment of the intensity of ground motions. The residual displacement gradualy increased after the pSv300 test, and increased in the opposite direction at the pSv420-1 test. In the pSv420-2 test, residual displacement remarkably increased from 250 mm to 1000 mm and the specimen collapsed at the middle of the pSv420-3 test.

3.2. Behavior of story

As an example of hysteretic behavior of collapsed story, Fig. 7 shows story shear force - drift angle relationship of the 2nd story. In the pSv110-1 test, a slight energy dissi-

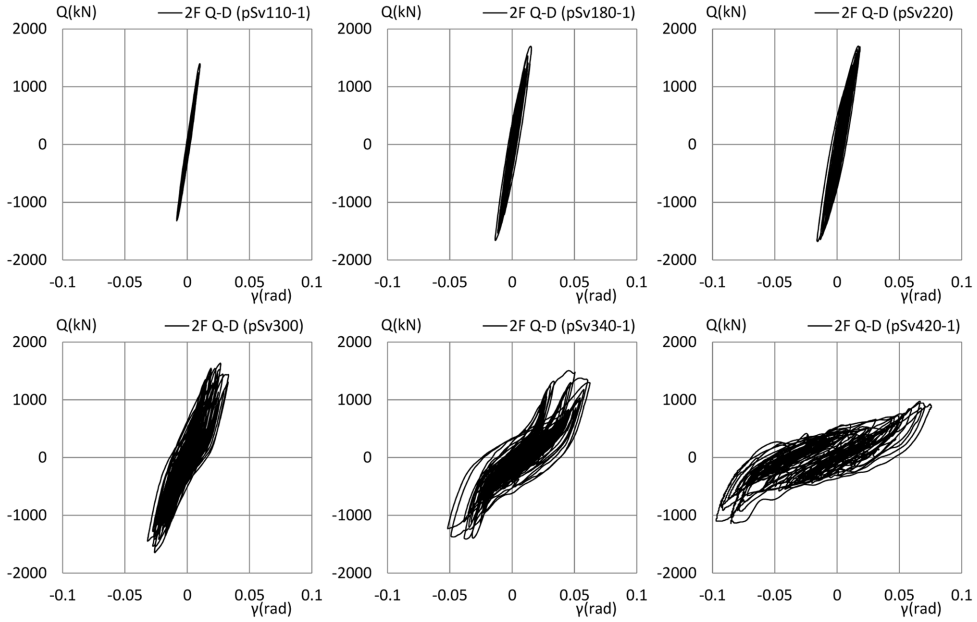


Figure 7. Story shear force - story drift angle relationship of the 2nd story.

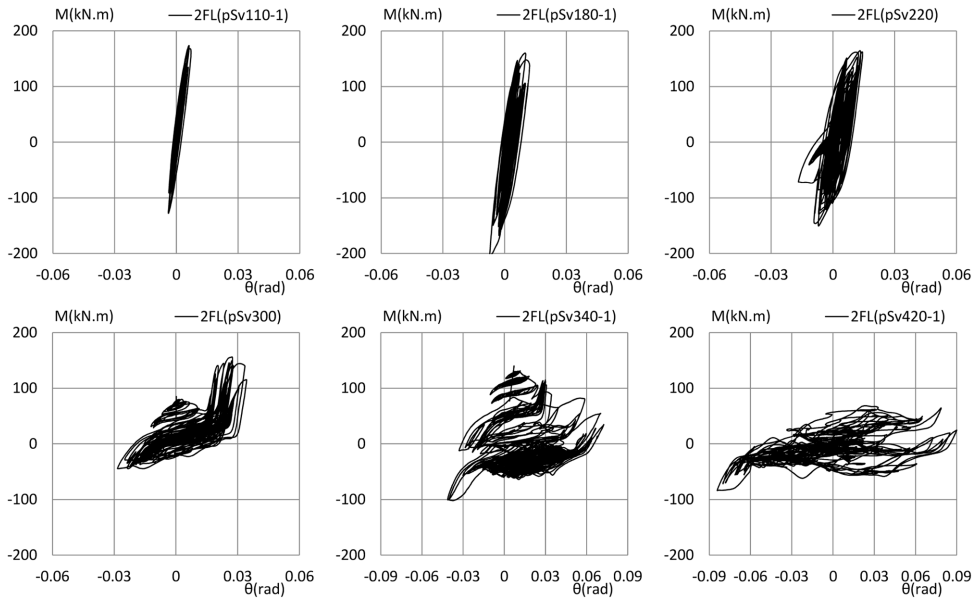


Figure 8. Moment - rotation relationship of B21 beam of the 2nd floor.



(a) beam end (b) bottom flange (c) top flange

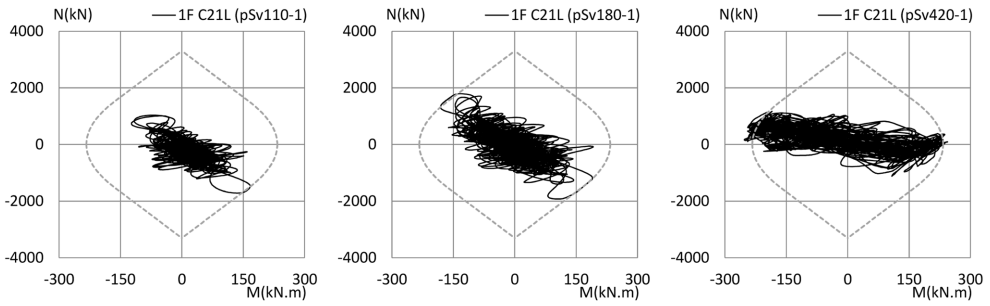
Figure 9. Fracture of beam end connection

pation by yielding of beams was observed. In the pSv180-1 test, the story shear force and the drift angle increased and the energy dissipation also increased. In the pSv220, inelastic sotry drift increased but the story shear force hardly increased. In the pSv300 test, deterioration was observed and the story shear force reduced during cyclic deformation of the story. The reduction of stiffness is observed around the zero story shear force and hysteretic loops showed pinching. In the pSv340-1 test, deterioration of story shear force was observed remarkably and pinching of the hysteretic loop become apparent. In the pSv420-1 test, story shear force deteriorated moreover and the recovery of the stiffness in large drift angle became negligible.

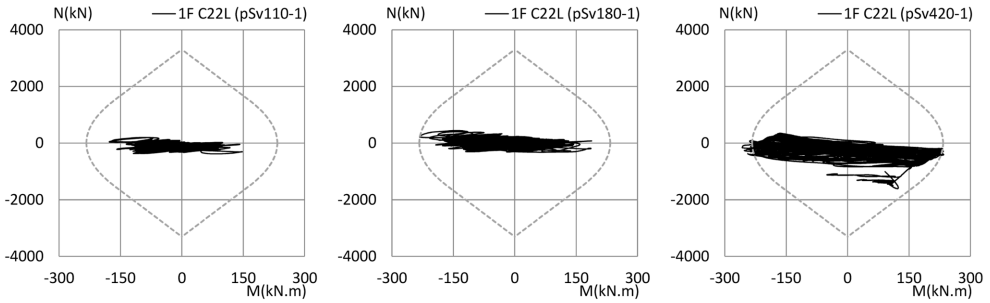
3.3. Behavior of beams

Since the specimen is designed by the weak beam - strong column criterion, yielding of the frame began at the beam end of the 2nd story. Fig. 8 shows moment - rotation relationship of the beam B21 connected with the exterior column C21 at the 2nd floor. In case of positive moment, the bottom flange of the beam subjected to compression force, conversely, subjected to tension force in case of negative moment. In the pSv110-1 test, the beam slightly yielded. In the pSv180-1 test, the moment increased to the full plastic moment (135 kN-m) and the loop expanded. In the pSv220 test, the moment deteriorated in negative moment due to fracture of the bottom flange. In the positive moment, the fractured flange contacted again and stiffness and strength recovered to almost initial state. In the pSv300 test, deterioration of negative moment was remarkable and recovery of moment in positive moment was limited in the large rotation. In the pSv340-1 tests, deterioration progressed and, in the pSv420-1 test, the recovery of moment hardly observed in both of positive and negative moment due to fracture of top and bottom flanges.

Fig. 9 shows fracture of the beam end after tests. The crack initiated from the toe of the weld access hole and propagated along the weld of the beam flange. In the pSv 420 tests, not only both of top and bottom flange but also



(a) Bottom end of C21 exterior column of the 1st story



(b) Bottom end of C22 interior column of the 1st story

Figure 10. Axial force N - bending moment M interaction of columns.

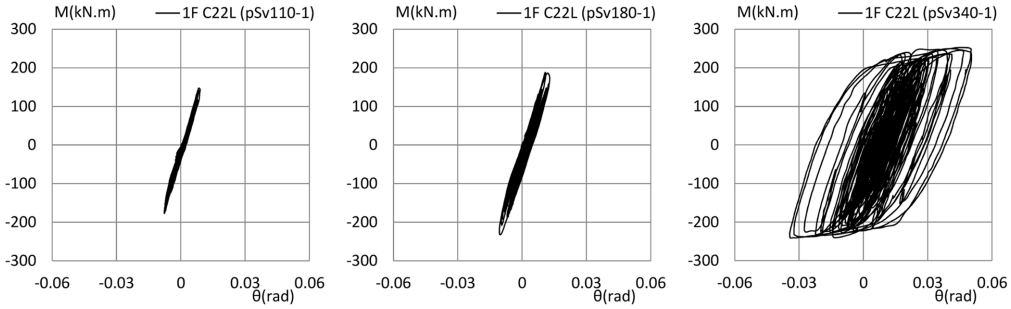


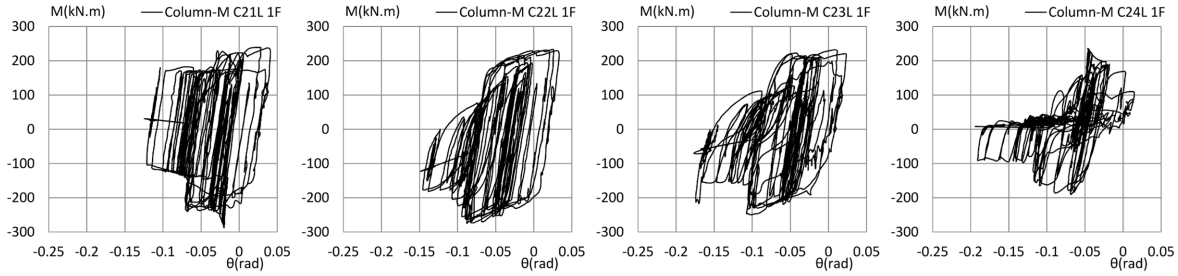
Figure 11. Moment - rotation relationship at the bottom of C22 interior column of the 1st atory.

the shear plate and high strength bolts fractured at the bolted web joint as shown in Fig. 9(a).

3.4. Behavior of columns

Fig. 10 shows the interaction between axial force N and bending moment M at the bottom of columns of the 1st story. The dotted lines shows the interaction curve of the yield of the square tube section. Fig. 10(a) shows the results of exterior column C21 whose axial force ratio n, which is defined as axial force devided by yield axial strength, was 0.12 by longtime load, and the maximum value of n during dynamic response was 0.58 in the pSv 180-1 test. The variation of axial force by dynamic response was large and the first yielding occurred under compressive axial force during the pSv110-1 test. In pSv 180-1 test, yielding occurred in both of tensile and compressive axial force. Fig. 10(b) shows the results of interior column C22 whose axial force ratio n was 0.16 in initial. The variation of axial force by dynamic response was smaller compaered with C21 and the influence of axial force on the full plastic strength was small.

After the pSv300 test, due to deterioration of story shear force as shown in Fig. 7, the variation of axial force became small. After the pSv420-1 test, the residual deformation of the frame occurred in the direction in which the column C21 and C22 subjected to tensile axial force and the column C23 and C24 subjected to compression axial force. Fig. 12 shows moment - rotation relationship at the bottom of columns of the 1st story in the pSv420-2 test. Column C21 and C22 show deterioration by fracture (Fig. 13(a)) and column C23 and C24 show deterioration by local buckling (Fig. 13(b)).



(a) C21 (b) C22 (c) C23 (d) C24

Figure 12. Moment - rotation relationship at the bottom of columns of the 1st story in pSv420-2 test.



(a) Fracture (b) Local buckling

Figrue 13. Damage to columns at the 1st story.

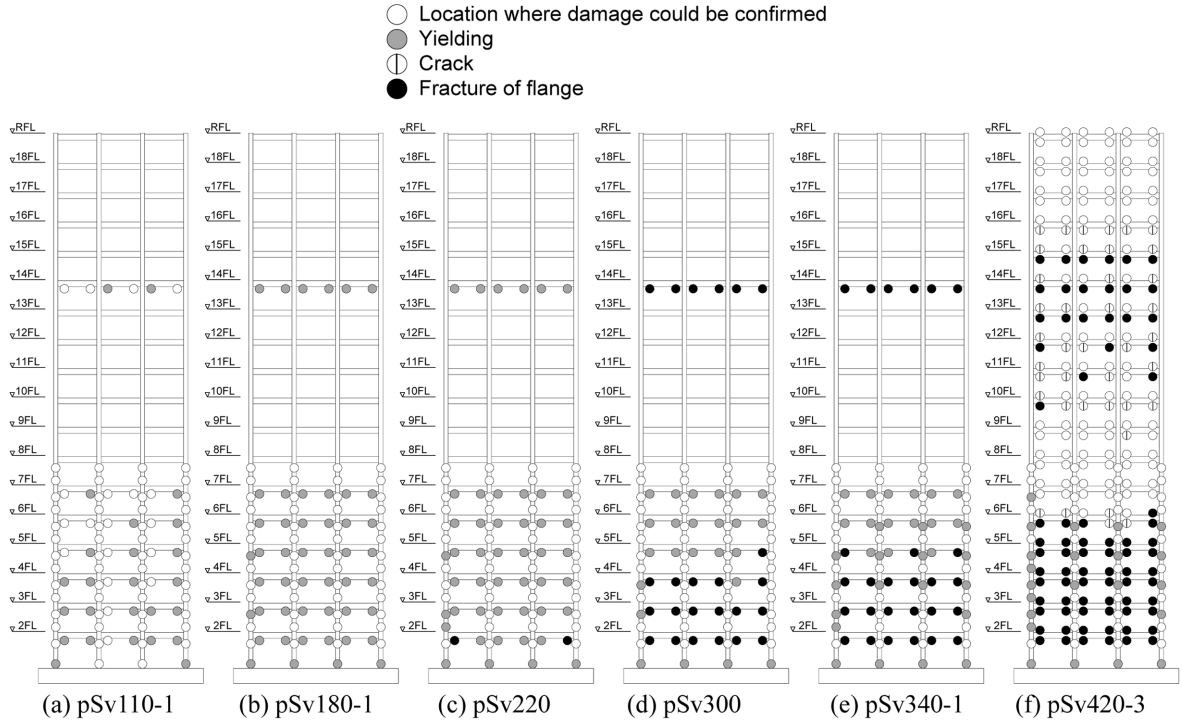
4. Damage to Frame

4.1. Damage to structural members

Fig. 14 shows damage to structural members, i.e., yielding and fracture of beams and yielding of columns. These damage are detected by video records, visual inspection and strains measured at the end of the members.

In the pSv110-1 test, some of beams yielded at the 2nd to 7th and 14th floor and, in the pSv180-1 test, all beams yielded at the same floor and the bending moment of some beams at the lower floor increased to the full plastic moment. From visual inspection after the pSv180-2 test, cracks were observed at the toe of weld access hole in the 2nd to 7th floor, especially at the beam end connected with the exterior columns.

Fracture of beam flanges initiated in the pSv220 test at the beam end connected to the exterior column of the 2nd floor and extended to the 3rd floor in the pSv250 test. At the same test, fracture of the bottom flanges were observed at the 14th floor. In the pSv300 test, all bottom flan-



(a) pSv110-1 (b) pSv180-1 (c) pSv220 (d) pSv300 (e) pSv340-1 (f) pSv420-3

Figure 14. Distribution of damage to beams and columns.

ges of the beams fractured at the 2nd and 3rd floor, and in the pSv340-1 test, some of the top flanges of the beams also fractured at the 2nd to 4th floor.

Yielding of columns were observed at the bottom end of the exterior column of the 1st story in the pSv110-1 test, at the bottom end of the interior columns of the 1st story and at the top end of the exterior columns of the 2nd and 4th floor in the pSv180-1 test. The local buckling of columns were observed in the pSv300 test.

4.2. Overall behavior during dynamic response

In order to examine the influence of fracture of beams on the overall behavior of the frame, moment diagram of the frame at the instant of the maximum drift occurred in each test are shown in Fig. 15.

In the pSv110-1 and pSv180-1 test, beams are in the state of double-curved flexure and columns above the 2nd floor are also in double-curved flexure. The bending moment at the bottom of the column of the 1st story were quite large because of fixed boundary condition.

In the pSv220 test, because of fracture of the bottom flanges at the end of beams connected with exterior columns, the bending moment of the beams connected with C24 column was reduced. On the contrary, at the beams connected with C21 column, the reduction of bending moment was not observed since the bottom flange was in compression.

In the pSv300 test, the reduction of bending moment at the beam end connected to C24 column extended to the 3rd floor. The reduction of beam end moment resulted in the change of moment diagram at C24 column, therefore the point of contraflexure at the 1st to the 3rd story of column is located only at the 3rd floor and elongation of the flexure length of the C24 column was observed in these stories.

In the pSv340-1 test, the elongation of the flexure length of C24 column extended to the 5th floor. Since fracture occurred at both of the top and bottom flanges of beam end, reduction of beam end moment was observed in C21 column and interior columns C22 and C23. Since elongation of the flexure length of columns extended to many columns and upper stories, shear forces of columns reduced in these stories.

In the pSv420-1 test, the elongation of the flexure length of columns was observed up to 7th floor and the shear forces carried by columns were reduced further.

4.3 Process to collapse

From foregoing obsevations of test results, the process to collapse of the specimen is as follows.

According to the weak beam - strong column criteria, a plastic mechanism by yielding of multistory beams and column base at the 1st story is formed.

Under long-duration ground motions, due to many cycles of repeated plastic deformation at beam ends, cracks initiate at the welds of beam bottom flanges and propagate along flange width followed by fracture of the bottom flange.

The area of fracture of beam flanges extends to the upper stories and fracture of beam flanges change moment diagram of columns. The flexure length of columns elongate to multistory and shear resistance of columns deteriorate.

Finally, at top ends and bottom ends of elongated flexure length of columns, plastic hinges formed and sidesway collapse occurred.

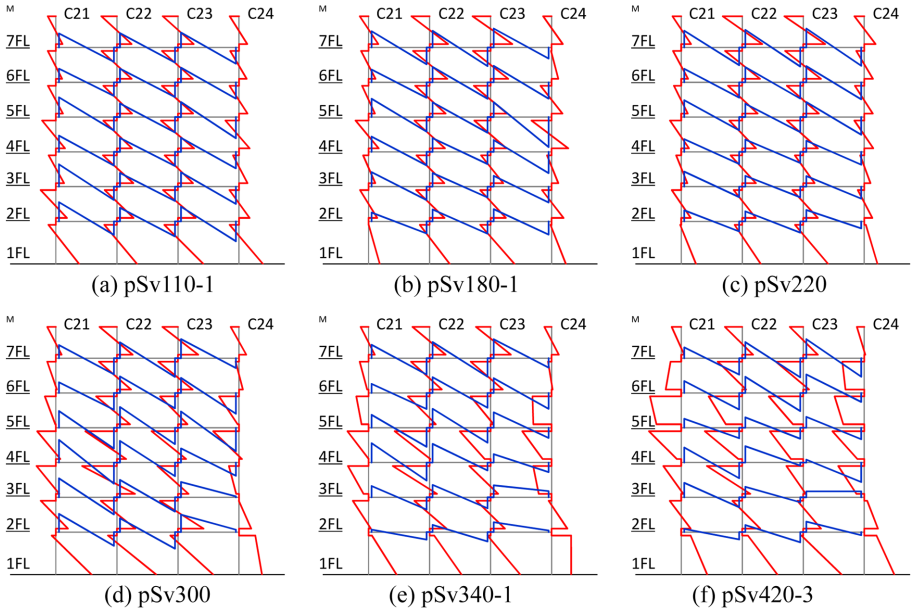


Figure 15. Moment diagram of the frame at the instant of maximum drift.

5. Conclusions

A series of shaking table tests of an 18-story steel moment resisting frame was conducted until total collapse of the frame by using synthetic long-period long-duration ground motions whose source is Nankai Trough Earthquake.

From test results, hysteretic characteristics of beams and columns including deterioration due to fracture and local buckling were revealed. The process to collapse of the frame was also examined.

From results obtained from the tests, accurate numerical simulation of collapse behavior of steel moment frames can be conducted in different conditions of the frame and ground motions.

Acknowledgement

This study is a part of "Special Project for the Maintenance and Recovery of Functionality in Urban Infrastructure" financed by MEXT in Japan, The team leader is Prof. Masayoshi Nakashima (Kyoto University, Japan). The test described in this paper is pursued by the subworking group of steel structure and the WG leader is Keiichiro Suita (Kyoto University). The authors acknowledge members of the WG, Dr. Yuji Koetaka (Kyoto University), Dr. Jun Iyama (Tokyo University), Dr. Takuya Nagae, Dr. Daiki Sato (NIED), Yoshikazu Sawamoto, Jun Kubota, Takatoki Kiyokawa (Kajima Technical Research Institute), Dr. Norihide Koshika (Kobori Research Complex Inc.) for their technical supports.

References

Suita, K., Nakashima, M., and Engelhardt, M. D. (2000). Comparison of Seismic Capacity between Post-Northridge and Post-Kobe Beam-to-Column Connections, *Proceedings of the Third International Conference on Behaviour of Steel Structures in Seismic Areas (STESSA)*, Montreal, Canada, pp. 271~278.

Suita, K., Takatsuka, K., and Tanaka, T. (2014). "Prediction of Fracture of Welded Moment Connection under Varying Amplitude Cyclic Loading," *Proceedings of the 2014 Structures Congress*, *ASCE*, pp. 2617~2628.

Kasai K., Pu W. C., and Wada A. (2012). "Responses of tall buildings in Tokyo during the 2011 great east Japan earthquake," *Proceedings of the Seventh International Conference on Behaviour of Steel Structures in Seismic Areas (STESSA)*, pp. 25~35.